

Supernova Neutrinos as a Precise Probe of Nuclear Neutron Skin

Xu-Run Huang¹ and Lie-Wen Chen^{1,*}

¹*School of Physics and Astronomy, Shanghai Key Laboratory for Particle Physics and Cosmology,
and Key Laboratory for Particle Astrophysics and Cosmology (MOE),
Shanghai Jiao Tong University, Shanghai 200240, China*

(Dated: December 12, 2022)

A precise and model-independent determination of the neutron distribution radius R_n and thus the neutron skin thickness R_{skin} of atomic nuclei is of fundamental importance in nuclear physics, particle physics and astrophysics but remains a big challenge in terrestrial labs. We argue that the nearby core-collapse supernova (CCSN) in our Galaxy may render a neutrino flux with unprecedentedly high luminosity, offering perfect opportunity to determine the R_n and R_{skin} through the coherent elastic neutrino-nucleus scattering (CE ν NS). We evaluate the potential of determining the R_n of lead (Pb) via CE ν NS with the nearby CCSN neutrinos in the RES-NOVA project which is designed to hunt CCSN neutrinos using an array of archaeological Pb based cryogenic detectors. We find that an ultimate precision of $\sim 0.1\%$ for the R_n (~ 0.006 fm for the R_{skin}) of Pb can be achieved via RES-NOVA in the most optimistic case that the CCSN explosion were to occur at a distance of ~ 1 kpc from the Earth.

I. INTRODUCTION

Neutrons are expected to be distributed more extensively than protons in heavy neutron-rich nuclei, forming a neutron skin which is featured quantitatively by the skin thickness $R_{\text{skin}} = R_n - R_p$ where R_n and R_p are the (point) neutron and proton rms radii of the nucleus, respectively. Theoretically, it has been established that the R_{skin} provides an ideal probe for the density dependence of the symmetry energy $E_{\text{sym}}(\rho)$ [1–15], which quantifies the isospin dependent part of the equation of state (EOS) for isospin asymmetric nuclear matter and plays a critical role in many issues of nuclear physics and astrophysics [16–27].

Experimentally, while the R_p can be precisely inferred from its corresponding charge rms radius R_{ch} which has been measured precisely via electromagnetic processes [28, 29], the R_n remains elusive since it is usually determined from strong processes, generally involving in model dependence (see, e.g., Ref. [30]). A clean approach to determine the R_n is to measure the parity-violating asymmetry A_{PV} in the elastic scattering of polarized electrons from the nucleus since the A_{PV} is particularly sensitive to the neutron distribution due to its large weak charge compared to the tiny one of the proton [31, 32]. Following this strategy, the ^{208}Pb radius experiment (PREX-2) [33] and ^{48}Ca radius experiment (CREX) [34] recently reported the determination of the R_n with a precision of $\sim 1\%$, i.e., $R_{\text{skin}}^{208} = 0.283 \pm 0.071$ fm for ^{208}Pb [33] and $R_{\text{skin}}^{48} = 0.121 \pm 0.026(\text{exp}) \pm 0.024(\text{model})$ fm for ^{48}Ca (1σ uncertainty). Very remarkably, analyses within modern energy density functionals [35–37] conclude a tension between the CREX and PREX-2 results, with the former favoring a very soft $E_{\text{sym}}(\rho)$ while the latter a very stiff one, calling for further critical theoretical and experimental investigations. Especially, the Bayesian analysis [37]

suggests that a higher precision for the R_n of ^{208}Pb is of particular importance to address this issue. The Mainz Radius Experiment (MREX) [38] is expected to shrink the uncertainty by a factor of two with a precision of 0.5% (or ± 0.03 fm) for the R_n of ^{208}Pb , but the experiment's start time is still largely uncertain [39].

Another clean and model-independent way to extract the R_{skin} is through the coherent elastic neutrino-nucleus scattering (CE ν NS) [40, 41], which was firstly observed by the COHERENT Collaboration via a CsI detector with the neutrino beam from the Spallation Neutron Source at Oak Ridge National Laboratory [42]. Based on the COHERENT data, the R_{skin} of CsI has been extracted [43, 44] but the uncertainty is too large to claim a determination, due to the low statistics of CE ν NS events. In nature, the nearby core-collapse supernova (CCSN) may render a neutrino flux with unprecedentedly high luminosity, which provides an excellent chance to explore CE ν NS. Indeed, detecting the next galactic SN neutrinos has received much attention both from large neutrino observatories and modern dark matter experiments [45–52]. One of the most powerful projects is the RES-NOVA experiment which will hunt CCSN neutrinos via CE ν NS by adopting an archaeological Pb based cryogenic detector [51, 52]. One merit of RES-NOVA is that using CE ν NS as its detection channel allows a flavor-blind neutrino measurement and thus avoids the uncertainties from the neutrino oscillation. The other merit is that archaeological Pb ensures the large CE ν NS cross section and the ultra-low levels of background, literally guaranteeing a high statistics.

In this work, we demonstrate that the very configuration of the RES-NOVA experiment provides an ideal site to determine the R_n of Pb, and an ultimate precision of $\sim 0.1\%$ for the R_n (~ 0.006 fm for the R_{skin}) of Pb can be achieved in the most optimistic case that the galactic CCSN would explode at a distance of ~ 1 kpc from the Earth. Even with a CCSN at 5 kpc, our present approach can still achieve a precision better than that from

* Corresponding author; lwchen@sjtu.edu.cn

PREX-2.

The paper is organized as follows. In Section II, we give a brief description of the supernova neutrinos. In Section III, we discuss the prospects of the neutrino detection in RES-NOVA experiment. In Section IV, the results on the neutron skin thickness sensitivity are presented and discussed. The conclusions are given in Section V.

II. SUPERNOVA NEUTRINOS

The detailed knowledge of a SN neutrino flux is still missing in experiments since we have only observed two dozen neutrino events from the SN 1987A [53, 54]. However, after three decades, current neutrino experiments have stepped into an era with unprecedented accuracy. The robust reconstruction of SN neutrino spectra with multiple detectors has been investigated [55–63] and an accurate measurement is promising for a nearby SN (e.g., < 5 kpc). Furthermore, modern SN simulations have achieved a tremendous progress in unveiling the mysteries of SN phenomena [64–68]. Based on current understanding, the spectral shape of CCSN neutrino fluxes for each flavor can be well approximated by a pinched thermal distribution [69, 70]

$$f_\nu(E_\nu) = A \left(\frac{E_\nu}{\langle E_\nu \rangle} \right)^\alpha \exp \left[-(\alpha + 1) \frac{E_\nu}{\langle E_\nu \rangle} \right]. \quad (1)$$

Here, E_ν and $\langle E_\nu \rangle$ are the neutrino energy and the averaged energy, α describes the amount of spectral pinching, and $A = \frac{(\alpha + 1)^{\alpha+1}}{\langle E_\nu \rangle \Gamma(\alpha + 1)}$ is the normalization constant, where Γ is the gamma function. So the neutrino fluence per flavor on the Earth from a CCSN at a distance d can be obtained as

$$\Phi(E_\nu) = \frac{1}{4\pi d^2} \frac{E_\nu^{\text{tot}}}{\langle E_\nu \rangle} f_\nu(E_\nu), \quad (2)$$

where E_ν^{tot} denotes the total emitted energy per flavor. In a real CCSN explosion, both the amounts and spectra of the emitted neutrinos change with time as the star evolves into different stages. However, to our goal, we only need information of total neutrino emission. Therefore, we adopt here the time-integrated neutrino emission parameters from a typical long-term axisymmetric CCSN simulation, which can be found in Table I of Ref. [58]. Note that although the neutrino emission of a CCSN also depends on the details of the transient, e.g., the progenitor mass, compactness, explosion dynamics, etc., it has a rough profile of $\langle E_\nu \rangle \sim 10$ MeV, $2 < \alpha < 4$ and $E^{\text{tot}} \sim 10^{53}$ erg. Nevertheless, the accurate information can be extracted from various detection data once a nearby CCSN explosion occurs.

III. DETECTION PROSPECTS IN RES-NOVA

To explore the potential of determining the R_n of Pb with RES-NOVA, we consider the RN-3 configuration in Table I of Ref. [51] which has a detector mass of 465 t and an energy threshold of 1 keV. The absorber with pure Pb is also adopted. For the detection channel, the differential cross section in the standard model has the form:

$$\frac{d\sigma}{dT}(E_\nu, T) = \frac{G_F^2 M}{4\pi} Q_W^2 F_W^2(q) \left[1 - \frac{T}{E_\nu} - \frac{MT}{2E_\nu^2} \right], \quad (3)$$

where G_F is the Fermi coupling constant; M denotes the mass of the target nucleus with $N(Z)$ neutrons (protons); Q_W is the weak charge and $F_W(q)$ is the weak form factor; E_ν and T represent the neutrino energy and the kinetic recoil energy of the nucleus, respectively; and the momentum transfer q is given by $q^2 \simeq 2MT$. Note Eq. (3) is for a nucleus with spin-0 and the result for a spin-1/2 target (i.e., ^{207}Pb in our case) will gain a tiny correction [71] which is neglected in this work.

The weak charge Q_W can be obtained as

$$Q_W = \int d^3r \rho_W(r) = Nq_n + Zq_p, \quad (4)$$

where $\rho_W(r)$ is the weak charge density. At tree level, the nucleon weak charges are $q_n = q_n^0 = 2g_V^n$ and $q_p = q_p^0 = 2g_V^p$, where the neutron (proton) vector coupling is defined as $g_V^n = -\frac{1}{2}$ ($g_V^p = \frac{1}{2} - 2\sin^2\theta_W$) with the low-energy weak mixing angle $\sin^2\theta_W = 0.23857(5)$ [72, 73]. In the present work, we adopt the values $q_n = -0.9878$ and $q_p = 0.0721$ to include radiative corrections [74]. The weak form factor $F_W(q)$ is expressed as

$$F_W(q) = \frac{1}{Q_W} \int d^3r \frac{\sin qr}{qr} \rho_W(r). \quad (5)$$

Here we use the Helm parametrization for the $F_W(q)$ [75, 76], which has been proven to be very successful for analyzing electron scattering form factors [77, 78]. The $F_W(q)$ is then expressed as

$$F_W(q) = 3 \frac{j_1(qR_0)}{qR_0} e^{-q^2 s^2/2}, \quad (6)$$

where $j_1(x) = \sin(x)/x^2 - \cos(x)/x$ is the spherical Bessel function of order one, R_0 is the diffraction radius and s quantifies the surface thickness. The rms radius R_W of weak charge density can then be obtained as

$$R_W^2 = \int d^3r \frac{r^2 \rho_W(r)}{Q_W} = \frac{3}{5} R_0^2 + 3s^2. \quad (7)$$

We use $s = 1.02$ fm following the discussion in Ref. [74]. The R_n and R_p are related to R_W and R_{ch} with the following relations [74, 79],

$$R_p^2 = R_{\text{ch}}^2 - \langle r_p^2 \rangle - \frac{N}{Z} \langle r_n^2 \rangle \quad (8)$$

and

$$R_n^2 = \frac{Q_W}{q_n N} R_W^2 - \frac{q_p Z}{q_n N} R_{\text{ch}}^2 - \langle r_p^2 \rangle - \frac{Z}{N} \langle r_n^2 \rangle + \frac{Z + N}{q_n N} \langle r_s^2 \rangle. \quad (9)$$

Here $\langle r_p^2 \rangle^{1/2} = 0.8414(19)$ fm [80] is the charge radius of a proton and $\langle r_n^2 \rangle = -0.1161(22)$ fm² [73] is that of a neutron, the squared strangeness radius of nucleon is taken to be $\langle r_s^2 \rangle = -0.0054(16)$ fm² according to Lattice QCD calculations [81, 82]. Note that the contributions of the Darwin-Foldy term and the spin-orbit current are neglected here since both of them are quite small and will not affect our conclusions on the relative precision evaluation of the R_n determination for Pb.

The archaeological Pb crystal in RES-NOVA is mainly composed of four isotopes, i.e., ^{204,206,207,208}Pb. The charge rms radius R_{ch} , the binding energies per nucleon E_B/A and the natural abundance Y_A of these isotopes can be found in Table I. Since it is impossible to distinguish the CE ν NS events from different isotopes in RES-NOVA, what we can extract from such detection is the averaged R_{skin} of Pb and that is what we really mean for the R_{skin} of Pb in this work. The mass of a nucleus is defined as $M = N \times m_n + Z \times m_p - E_B$ where E_B is the binding energy and $m_{n(p)}$ is the rest mass of neutrons(protons).

We first assume a constant 100% acceptance efficiency in the detector, and the expected event counts can then be obtained as

$$\frac{dN}{dT} = \sum Y_A N_t \int_{E_{\text{min}}} dE_\nu \Phi(E_\nu) \frac{d\sigma}{dT}(E_\nu, T). \quad (10)$$

Here, $N_t = N_A m_{\text{det}}/M_{\text{Pb}}$ is the number of nuclei in the crystals with N_A being the Avogadro constant, m_{det} the detector mass and $M_{\text{Pb}} = 0.2072$ kg/mol the molar mass of Pb. Strictly speaking, the value of E_{min} depends on T due to the relation: $T_{\text{max}} = 2E_\nu^2/(M + 2E_\nu)$. We adopt $T_{\text{max}} \simeq 2E_\nu^2/M$ since $M \gg E_\nu$ in this scattering. The final count will sum over both the isotopes and neutrino flavors, and integrate over the corresponding energy bin.

The final result will vitally depend on the distance of the SN. On the one hand, the target SN cannot be too far since the event rate has an inverse quadratic dependence on the distance, as shown in Eq. (2) and Eq. (10). Especially, the relative high energy part ($T > 10$ keV) has rather low event rate and even gets hidden under the background for $d = 10$ kpc [51]. However, recent study shows there exists shock acceleration in SN to create more

TABLE I. Charge radii R_{ch} [29], binding energies per nucleon E_B/A [83] and abundance Y_A [84] of Pb isotopes.

Isotopes	R_{ch} (fm)	E_B/A (MeV)	Y_A
204	5.4803(14)	7.87993	0.014(6)
206	5.4902(14)	7.87536	0.241(30)
207	5.4943(14)	7.86987	0.221(50)
208	5.5012(13)	7.86745	0.524(70)

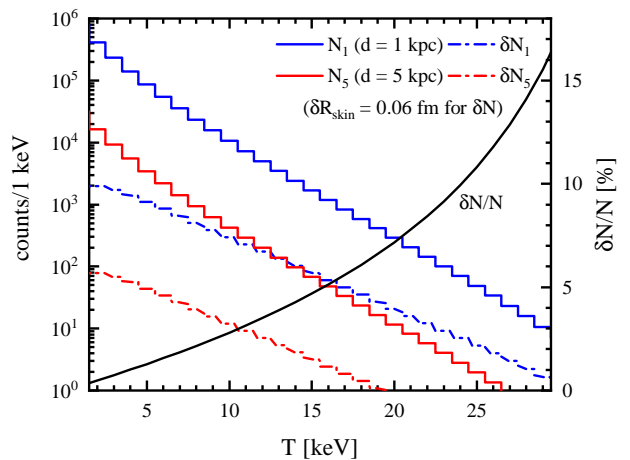


FIG. 1. The predicted event counts per 1 keV versus nuclear kinetic recoil energy T at the RES-NOVA detector for a SN at 1 kpc (N_1 , blue solid line) and 5 kpc (N_5 , red solid line), using the PREX-2 result as the averaged R_{skin} of Pb. The dashed lines (δN_1 and δN_5) show the change amplitude of counts with a 0.06 fm variation of the neutron skin thickness. The relative variation $\delta N/N$ of the counts is given for both SN distances by the black line (right axis).

high energy heavy flavor neutrinos [85]. Note that the nucleon distribution radii exhibit stronger sensitivity to the form factor at higher momentum transfer in this low energy range. We thus choose $d = 5$ kpc for a typically far distance SN target. On the other hand, a very nearby SN will lead to a neutrino flux intense enough to cause signal pile-up in the detector. This phenomenon has been studied recently by the RES-NOVA Collaboration, and the results show that the pile-up probability will decrease to almost zero for $d \gtrsim 1$ kpc [52]. Therefore, $d = 1$ kpc turns out to be an optimal choice.

The expected results are shown in Fig. 1. We adopt an energy bin of 1 keV, which is allowable since the energy resolution of RES-NOVA is expected to be 0.2 keV. The statistics is promising for both cases of $d = 1$ kpc and $d = 5$ kpc. In particular, the count per bin ranges from 10^3 to 10^5 in the recoil energy range (3 – 19 keV) for a SN at 1 kpc, while it becomes approximately one order of magnitude smaller for $d = 5$ kpc. We also estimate the sensitivity to the variation of the R_{skin} . As an example, we plot the count change for a R_{skin} variation of 0.06 fm ($\sim 1\%$). The modifications on counts for $d = 1(5)$ kpc stay within about $10^1(1) - 10^3(10^2)$ depending on the recoil energy T . To elucidate this effect more clearly, the relative difference $\delta N/N$ is also shown by the black line. As anticipated, the $\delta N/N$ only depends on the recoil energy for a certain variation of the R_{skin} and increases with the recoil energy. This is because it directly quantifies the modifications on the form factor. On the other hand, one sees that both the expected counts and its variation δN decrease exponentially with the recoil energy. This is due to the roughly exponential decay of SN neutrino flux as a function of neutrino energy at higher energies as shown in

Eq. (1). As a result, considering both the sensitivity and event statistics, the bins around the center ($T \sim 15$ keV) are more suitable to measure the R_{skin} .

IV. NEUTRON SKIN THICKNESS SENSITIVITY

In order to carry out a statistical evaluation on the precision of the R_n determination, we follow Ref. [86] and adopt the following chi-squares function:

$$\chi^2 = \sum_{\text{bins}} \frac{(N_{\text{exp}} - N_{\text{th}})^2}{\sigma_{\text{stat}}^2 + \sigma_{\text{syst}}^2}. \quad (11)$$

Here, the ‘‘experimental’’ data N_{exp} is taken as the expected counts with $R_{\text{skin}} = 0.283$ fm and the theoretical counts N_{th} will vary according to the R_{skin} value. Except for the statistical uncertainty $\sigma_{\text{stat}} = \sqrt{N_{\text{exp}}}$, we also introduce an effective systematic error $\sigma_{\text{syst}} = pN_{\text{th}}/100$ to quantify the possible uncertainties originating from the future RES-NOVA detector, the extracted SN neutrino spectra from other detection, and so on, with p representing the percentage of the future systematic error. The sum in Eq. (11) only runs over the energy bins around the center part at $T \sim 15$ keV (see the following for the detailed values). For bins with lower energy, they have higher statistics but much less sensitivity to the neutron form factor due to their almost full coherence. Moreover, the previous assumption of an energy-independent 100% acceptance efficiency is more likely to become unacceptable in the energy bins near the threshold of detector. We thus drop the first 3 bins above the energy threshold and choose the minimum recoil energy to be $T_{\text{min}} = 4.5$ keV, which corresponds to a minimum neutrino energy of $E_{\text{min}} \simeq 20.9$ MeV. That means that only the high energy SN neutrinos contribute to this analysis. In contrast, bins in higher energy region show better sensitivity but poor statistics. We adopt $T_{\text{max}} = 29.5(20.5)$ keV [corresponding to a minimum neutrino energy of $E_{\text{min}} \simeq 53.4(44.6)$ MeV] for $d = 1(5)$ kpc just to ensure that every bins have a reasonable event number (i.e. $N > 10$).

The resulting χ^2 as a function of the variation δR_{skin} for the neutron skin thickness is shown in Fig. 2 where the future systematic error is presumed to be 1% or 5%. In particular, the 1σ uncertainty for a 1(5)% systematic error is $\pm 0.008(0.016)$ fm if the SN is located at $d = 1$ kpc, and $\pm 0.030(0.044)$ fm at $d = 5$ kpc. It is remarkable that our approach can achieve an ultimate precision of $\sim 0.1\%$ in the optimal case of $d = 1$ kpc, even much higher than the expected precision of the future MREX [38].

The systematic error σ_{syst} is of great importance in future experiments and observations, and our current knowledge on σ_{syst} is rather insufficient. To see more clearly how the precision depends on the σ_{syst} , we plot in Fig. 3 the expected 1σ precision (in percentage) for the R_n determination as a function of the σ_{syst} . It is seen

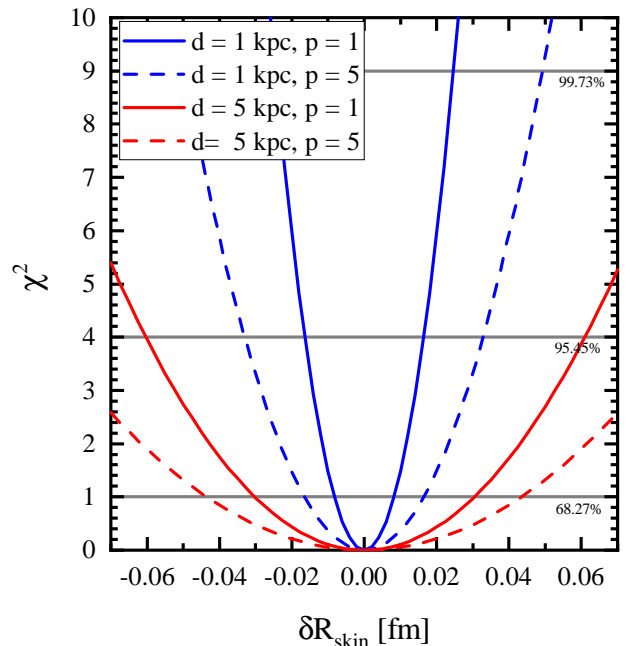


FIG. 2. The expected sensitivity to the variation of neutron skin thickness δR_{skin} for a SN at 1 kpc (blue lines) and 5 kpc (red lines) with 1% (solid lines) and 5% (dashed lines) systematic error.

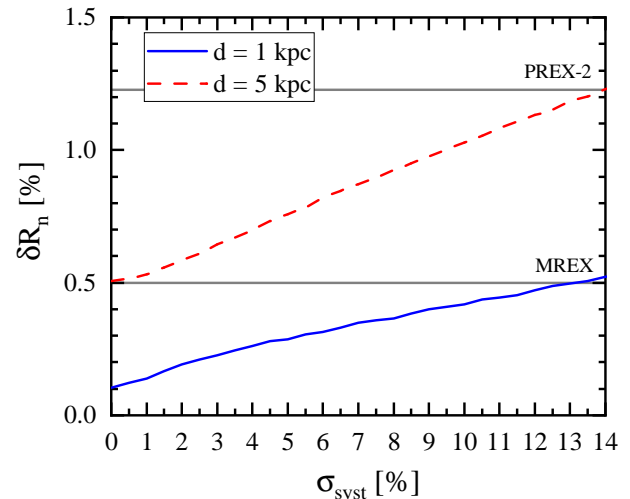


FIG. 3. The expected precision of the averaged neutron radius R_n (in percent) as a function of the systematic uncertainty for a 1 kpc (blue solid line) and 5 kpc (red dashed line) SN. The results from PREX-2 [33] and the future MREX [38] are also included for comparison.

that the σ_{syst} dependence is nearly unaffected by the SN distance and is almost linear. Generally, the closer the SN is located, the better its neutrino flux can be measured, and thus the smaller σ_{syst} from the spectra will be achieved. In particular, the determination of the R_n can achieve a precision better than that of MREX for a

nearby SN at $d \simeq 1$ kpc as long as $\sigma_{\text{sys}} \lesssim 13\%$ as shown in Fig. 3. Even under a worse condition at $d \simeq 5$ kpc, one can still anticipate a precision better than that of PREX-2. At this point, we would like to emphasize that the nearby presupernova stars are not too rare in our Galaxy. For example, a list of 31 candidates within 1 kpc, including the famous Betelgeuse, can be found in Ref. [87]. Accordingly, more than ~ 750 candidates are expected to exist in $1 \sim 5$ kpc assuming the presupernova stars are uniformly distributed around the Earth in the Milky Way Disk. In addition, assuming the CCSN rate is about 2 per 100 years in our Galaxy and the rate is further assumed to be uniform for a rough estimate, one then obtains a rate of $2 \times (5 \text{ kpc}/15 \text{ kpc})^2 \approx 0.2$ per 100 years within 5 kpc. On the other hand, it is very interesting to note that there are totally six galactic SNe which have been recorded so far since 1000 A.D., i.e., Lupus at 2.2 kpc in 1006 (SN 1006), Crab at 2.0 kpc in 1054 (SN 1054), 3C 58 at 2.6 kpc in 1181 (SN 1181), Tycho at 2.4 kpc in 1572 (SN 1572), Kepler at 4.2 kpc in 1604 (SN 1604), and Cas A at 2.92 kpc in 1680 (SN 1680), and they all occurred within 5 kpc from the Earth [88]. Among the six galactic SNe, four of them, namely, Crab (SN 1054), 3C 58 (SN 1181), Kepler (SN1604) and Cas A (SN 1680) were considered to be created by CCSNe [88]. However, it should be noted that more recent studies indicate the Kepler (SN1604) seems to be now generally regarded to have been a type Ia supernova, although a surviving donor has not been detected (see, e.g., Ref. [89]). Therefore, there are at least three recorded CCSNe (i.e., SN 1054, SN 1181 and SN 1680) so far within 5 kpc from the Earth since 1000 A.D.. In particular, the most recent recorded CCSN, i.e., Cas A, occurred more than 340 years ago (in 1680) [88]. Based on these observations, we conclude that while it is hard to predict precisely when the next nearby CCSN would occur, one may still expect optimistically that the nearby ($\lesssim 5$ kpc) CCSN seems to be imminent.

Furthermore, it is instructive to have a discussion on the measurement of ν spectra from a CCSN since it contributes to σ_{sys} . For a flavor-blind measurement of ν spectra for our present motivation, one only needs to know the configuration of total ν flux (ν^0) when they are freshly produced in the CCSN. At this initial stage, heavy flavor neutrinos (ν_x^0 and $\bar{\nu}_x^0$ with $x = \mu, \tau$) contribute to the total ν^0 flux by $\sim 2/3$ with the neutrinos and their anti-neutrinos having equal fraction ($\nu_x^0 = \bar{\nu}_x^0$), while ν_e^0 and $\bar{\nu}_e^0$ contribute to the rest $\sim 1/3$. However, the neutrino flavor conversions will occur during the neutrinos propagate before they eventually reach terrestrial detectors. Assuming adiabatic conversion in the SN, in the case of the normal mass ordering, the observed luminosity of a neutrino species $L_{\nu_i}^{\text{obs}}$ is [90]

$$L_{\nu_e}^{\text{obs}} = L_{\nu_x^0}, \quad (12)$$

$$L_{\bar{\nu}_e}^{\text{obs}} = \cos^2\theta_{12}L_{\bar{\nu}_e^0} + \sin^2\theta_{12}L_{\bar{\nu}_x^0}, \quad (13)$$

where θ_{12} is the mixing angle between mass eigenstates ν_1 and ν_2 . In the case of the inverted mass ordering, the observed luminosity of a neutrino species $L_{\nu_i}^{\text{obs}}$ is [90]

$$L_{\nu_e}^{\text{obs}} = \sin^2\theta_{12}L_{\nu_e^0} + \cos^2\theta_{12}L_{\nu_x^0}, \quad (14)$$

$$L_{\bar{\nu}_e}^{\text{obs}} = L_{\bar{\nu}_e^0}. \quad (15)$$

Therefore, after the neutrino flavor conversions, the ν_x^0 or $\bar{\nu}_x^0$ spectra can be determined from the signals of ν_e (e.g., DUNE [48]) or $\bar{\nu}_e$ (e.g., Hyper-K [50]), respectively, for a given neutrino mass ordering (i.e., $\nu_e = \nu_x^0$ for normal mass ordering while $\bar{\nu}_e = \bar{\nu}_x^0$ for inverted mass ordering). On the other hand, after the neutrino flavor conversions, for normal (inverted) mass ordering, the spectra of $\bar{\nu}_e^0$ (ν_e^0) (roughly $\sim 1/6$ in ν^0) can be extracted from the $\bar{\nu}_e$ (ν_e) signals while information of ν_e^0 ($\bar{\nu}_e^0$) is only carried by ν_x ($\bar{\nu}_x$) signals which can be measured by dark matter detectors [49] or other neutral current detectors (e.g., JUNO [47]).

Finally, we would like to mention that the advanced ab initio approaches using nuclear forces from chiral effective field theory can now describe the properties of heavy nuclei such as ^{208}Pb [91]. In particular, the ab initio calculations predict $R_{\text{skin}}^{48} = 0.141 - 0.187$ fm and $R_{\text{skin}}^{208} = 0.139 - 0.200$ fm [91], consistent with the CREX result of $R_{\text{skin}}^{48} = 0.121 \pm 0.026(\text{exp}) \pm 0.024(\text{model})$ fm [34] but exhibiting a mild tension with the PREX-2 result of $R_{\text{skin}}^{208} = 0.283 \pm 0.071$ fm [33]. The approach proposed in the present work with the expected high precision for the R_{skin}^{208} determination can thus crosscheck the PREX-2 result and test the ab initio prediction on R_{skin}^{208} . In addition, our approach in principle can be also applied to determine the R_{skin} of other nuclei which are adopted as large-scale detector medium to hunt dark matter and neutrinos, e.g., Xe isotopes in next-generation xenon-based detector [92].

V. CONCLUSIONS

We have demonstrated that the neutrinos from a nearby CCSN in our Galaxy can be used to precisely determine the R_n and R_{skin} of Pb via CE ν NS in RES-NOVA. In particular, an ultimate precision of $\sim 0.1\%$ (~ 0.006 fm) for the R_n (R_{skin}) of Pb is expected to be achieved in the most optimistic case that the CCSN explosion were to occur at a distance of ~ 1 kpc from the Earth. Such a precision of the R_{skin} is significantly higher than that of the existing and planned experiments in terrestrial labs, and will eventually pin down the density dependence of the symmetry energy and clarify the issue of the tension between CREX and PREX-2 experiments.

ACKNOWLEDGMENTS

The authors thank Ning Zhou for useful discussions. This work was supported by the National SKA Program of China No. 2020SKA0120300 and the National Natural Science Foundation of China under Grant Nos. 12235010 and 11625521.

-
- [1] B. A. Brown, *Phys. Rev. Lett.* **85**, 5296 (2000).
- [2] S. Typel and B. A. Brown, *Phys. Rev. C* **64**, 027302 (2001).
- [3] R. J. Furnstahl, *Nucl. Phys. A* **706**, 85 (2002), [arXiv:nucl-th/0112085](#).
- [4] S. Yoshida and H. Sagawa, *Phys. Rev. C* **69**, 024318 (2004).
- [5] L.-W. Chen, C. M. Ko, and B.-A. Li, *Phys. Rev. C* **72**, 064309 (2005), [arXiv:nucl-th/0509009](#).
- [6] M. Centelles, X. Roca-Maza, X. Vinas, and M. Warda, *Phys. Rev. Lett.* **102**, 122502 (2009), [arXiv:0806.2886 \[nucl-th\]](#).
- [7] L.-W. Chen, C. M. Ko, B.-A. Li, and J. Xu, *Phys. Rev. C* **82**, 024321 (2010), [arXiv:1004.4672 \[nucl-th\]](#).
- [8] P. G. Reinhard and W. Nazarewicz, *Phys. Rev. C* **81**, 051303 (2010), [arXiv:1002.4140 \[nucl-th\]](#).
- [9] X. Roca-Maza, M. Centelles, X. Vinas, and M. Warda, *Phys. Rev. Lett.* **106**, 252501 (2011), [arXiv:1103.1762 \[nucl-th\]](#).
- [10] B. K. Agrawal, J. N. De, and S. K. Samaddar, *Phys. Rev. Lett.* **109**, 262501 (2012), [arXiv:1212.0292 \[nucl-th\]](#).
- [11] Z. Zhang and L.-W. Chen, *Phys. Lett. B* **726**, 234 (2013), [arXiv:1302.5327 \[nucl-th\]](#).
- [12] C. Mondal, B. K. Agrawal, M. Centelles, G. Colò, X. Roca-Maza, N. Paar, X. Viñas, S. K. Singh, and S. K. Patra, *Phys. Rev. C* **93**, 064303 (2016), [arXiv:1605.05048 \[nucl-th\]](#).
- [13] A. R. Raduta and F. Gulminelli, *Phys. Rev. C* **97**, 064309 (2018), [arXiv:1712.05973 \[nucl-th\]](#).
- [14] W. G. Newton and G. Crocombe, *Phys. Rev. C* **103**, 064323 (2021), [arXiv:2008.00042 \[nucl-th\]](#).
- [15] W. G. Lynch and M. B. Tsang, *Phys. Lett. B* **830**, 137098 (2022), [arXiv:2106.10119 \[nucl-th\]](#).
- [16] P. Danielewicz, R. Lacey, and W. G. Lynch, *Science* **298**, 1592 (2002), [arXiv:nucl-th/0208016](#).
- [17] J. M. Lattimer and M. Prakash, *Science* **304**, 536 (2004), [arXiv:astro-ph/0405262](#).
- [18] A. W. Steiner, M. Prakash, J. M. Lattimer, and P. J. Ellis, *Phys. Rept.* **411**, 325 (2005), [arXiv:nucl-th/0410066](#).
- [19] V. Baran, M. Colonna, V. Greco, and M. Di Toro, *Phys. Rept.* **410**, 335 (2005), [arXiv:nucl-th/0412060](#).
- [20] B.-A. Li, L.-W. Chen, and C. M. Ko, *Phys. Rept.* **464**, 113 (2008), [arXiv:0804.3580 \[nucl-th\]](#).
- [21] C. J. Horowitz, E. F. Brown, Y. Kim, W. G. Lynch, R. Michaels, A. Ono, J. Piekarewicz, M. B. Tsang, and H. H. Wolter, *J. Phys. G* **41**, 093001 (2014), [arXiv:1401.5839 \[nucl-th\]](#).
- [22] S. Gandolfi, A. Gezerlis, and J. Carlson, *Ann. Rev. Nucl. Part. Sci.* **65**, 303 (2015), [arXiv:1501.05675 \[nucl-th\]](#).
- [23] F. Özel and P. Freire, *Ann. Rev. Astron. Astrophys.* **54**, 401 (2016), [arXiv:1603.02698 \[astro-ph.HE\]](#).
- [24] M. Baldo and G. F. Burgio, *Prog. Part. Nucl. Phys.* **91**, 203 (2016), [arXiv:1606.08838 \[nucl-th\]](#).
- [25] X. Roca-Maza and N. Paar, *Prog. Part. Nucl. Phys.* **101**, 96 (2018), [arXiv:1804.06256 \[nucl-th\]](#).
- [26] C. Drischler, J. W. Holt, and C. Wellenhofer, *Ann. Rev. Nucl. Part. Sci.* **71**, 403 (2021), [arXiv:2101.01709 \[nucl-th\]](#).
- [27] B.-A. Li, B.-J. Cai, W.-J. Xie, and N.-B. Zhang, *Universe* **7**, 182 (2021), [arXiv:2105.04629 \[nucl-th\]](#).
- [28] G. Fricke, C. Bernhardt, K. Heilig, L. A. Schaller, L. Schellenberg, E. B. Shera, and C. W. de Jager, *Atom. Data Nucl. Data Tabl.* **60**, 177 (1995).
- [29] I. Angeli and K. P. Marinova, *Atom. Data Nucl. Data Tabl.* **99**, 69 (2013).
- [30] M. Thiel, C. Sienti, J. Piekarewicz, C. J. Horowitz, and M. Vanderhaeghen, *J. Phys. G* **46**, 093003 (2019), [arXiv:1904.12269 \[nucl-ex\]](#).
- [31] T. W. Donnelly, J. Dubach, and I. Sick, *Nucl. Phys. A* **503**, 589 (1989).
- [32] C. J. Horowitz, S. J. Pollock, P. A. Souder, and R. Michaels, *Phys. Rev. C* **63**, 025501 (2001), [arXiv:nucl-th/9912038](#).
- [33] D. Adhikari *et al.* (PREX), *Phys. Rev. Lett.* **126**, 172502 (2021), [arXiv:2102.10767 \[nucl-ex\]](#).
- [34] D. Adhikari *et al.* (CREX), *Phys. Rev. Lett.* **129**, 042501 (2022), [arXiv:2205.11593 \[nucl-ex\]](#).
- [35] P.-G. Reinhard, X. Roca-Maza, and W. Nazarewicz, (2022), [arXiv:2206.03134 \[nucl-th\]](#).
- [36] E. Yüksel and N. Paar, (2022), [arXiv:2206.06527 \[nucl-th\]](#).
- [37] Z. Zhang and L.-W. Chen, (2022), [arXiv:2207.03328 \[nucl-th\]](#).
- [38] D. Becker *et al.*, *Eur. Phys. J. A* **54**, 208 (2018), [arXiv:1802.04759 \[nucl-ex\]](#).
- [39] C. Middleton, *Physics Today* **74**, 12 (2021).
- [40] D. Z. Freedman, *Phys. Rev. D* **9**, 1389 (1974).
- [41] D. Z. Freedman, D. N. Schramm, and D. L. Tubbs, *Ann. Rev. Nucl. Part. Sci.* **27**, 167 (1977).
- [42] D. Akimov *et al.* (COHERENT), *Science* **357**, 1123 (2017), [arXiv:1708.01294 \[nucl-ex\]](#).
- [43] M. Cadeddu, C. Giunti, Y. F. Li, and Y. Y. Zhang, *Phys. Rev. Lett.* **120**, 072501 (2018), [arXiv:1710.02730 \[hep-ph\]](#).
- [44] X.-R. Huang and L.-W. Chen, *Phys. Rev. D* **100**, 071301 (2019), [arXiv:1902.07625 \[hep-ph\]](#).
- [45] K. Scholberg, *Ann. Rev. Nucl. Part. Sci.* **62**, 81 (2012), [arXiv:1205.6003 \[astro-ph.IM\]](#).
- [46] J. Aalbers *et al.* (DARWIN), *JCAP* **11**, 017 (2016), [arXiv:1606.07001 \[astro-ph.IM\]](#).
- [47] F. An *et al.* (JUNO), *J. Phys. G* **43**, 030401 (2016), [arXiv:1507.05613 \[physics.ins-det\]](#).
- [48] B. Abi *et al.* (DUNE), *Eur. Phys. J. C* **81**, 423 (2021), [arXiv:2008.06647 \[hep-ex\]](#).
- [49] P. Agnes *et al.* (DarkSide 20k), *JCAP* **03**, 043 (2021), [arXiv:2011.07819 \[astro-ph.HE\]](#).
- [50] K. Abe *et al.* (Hyper-Kamiokande), *Astrophys. J.* **916**, 15 (2021), [arXiv:2101.05269 \[astro-ph.IM\]](#).
- [51] L. Pattavina, N. Ferreiro Iachellini, and I. Tamborra, *Phys. Rev. D* **102**, 063001 (2020), [arXiv:2004.06936 \[astro-ph.HE\]](#).
- [52] L. Pattavina *et al.* (RES-NOVA), *JCAP* **10**, 064 (2021), [arXiv:2103.08672 \[astro-ph.IM\]](#).
- [53] R. M. Bionta *et al.*, *Phys. Rev. Lett.* **58**, 1494 (1987).
- [54] K. Hirata *et al.* (Kamiokande-II), *Phys. Rev. Lett.* **58**, 1490 (1987).
- [55] H. Minakata, H. Nunokawa, R. Tomas, and J. W. F. Valle, *JCAP* **12**, 006 (2008), [arXiv:0802.1489 \[hep-ph\]](#).
- [56] B. Dasgupta and J. F. Beacom, *Phys. Rev. D* **83**, 113006 (2011), [arXiv:1103.2768 \[hep-ph\]](#).

- [57] J.-S. Lu, Y.-F. Li, and S. Zhou, *Phys. Rev. D* **94**, 023006 (2016), arXiv:1605.07803 [hep-ph].
- [58] A. Nikrant, R. Laha, and S. Horiuchi, *Phys. Rev. D* **97**, 023019 (2018), arXiv:1711.00008 [astro-ph.HE].
- [59] A. Gallo Rosso, F. Vissani, and M. C. Volpe, *JCAP* **04**, 040 (2018), arXiv:1712.05584 [hep-ph].
- [60] H.-L. Li, Y.-F. Li, M. Wang, L.-J. Wen, and S. Zhou, *Phys. Rev. D* **97**, 063014 (2018), arXiv:1712.06985 [hep-ph].
- [61] H.-L. Li, X. Huang, Y.-F. Li, L.-J. Wen, and S. Zhou, *Phys. Rev. D* **99**, 123009 (2019), arXiv:1903.04781 [hep-ph].
- [62] A. Gallo Rosso, *JCAP* **06**, 046 (2021), arXiv:2012.12579 [hep-ph].
- [63] H. Nagakura, *Mon. Not. Roy. Astron. Soc.* **500**, 319 (2020), arXiv:2008.10082 [astro-ph.HE].
- [64] H. T. Janka, T. Melson, and A. Summa, *Ann. Rev. Nucl. Part. Sci.* **66**, 341 (2016), arXiv:1602.05576 [astro-ph.SR].
- [65] B. Müller, *Publ. Astron. Soc. Austral.* **33**, e048 (2016), arXiv:1608.03274 [astro-ph.SR].
- [66] O. Just, R. Bollig, H.-T. Janka, M. Obergaulinger, R. Glas, and S. Nagataki, *Mon. Not. Roy. Astron. Soc.* **481**, 4786 (2018), arXiv:1805.03953 [astro-ph.HE].
- [67] E. O'Connor *et al.*, *J. Phys. G* **45**, 104001 (2018), arXiv:1806.04175 [astro-ph.HE].
- [68] H. Nagakura, A. Burrows, D. Vartanyan, and D. Radice, *Mon. Not. Roy. Astron. Soc.* **500**, 696 (2020), arXiv:2007.05000 [astro-ph.HE].
- [69] M. T. Keil, G. G. Raffelt, and H.-T. Janka, *Astrophys. J.* **590**, 971 (2003), arXiv:astro-ph/0208035.
- [70] I. Tamborra, B. Müller, L. Hudepohl, H.-T. Janka, and G. Raffelt, *Phys. Rev. D* **86**, 125031 (2012), arXiv:1211.3920 [astro-ph.SR].
- [71] M. Lindner, W. Rodejohann, and X.-J. Xu, *JHEP* **03**, 097 (2017), arXiv:1612.04150 [hep-ph].
- [72] K. S. Kumar, S. Mantry, W. J. Marciano, and P. A. Souder, *Ann. Rev. Nucl. Part. Sci.* **63**, 237 (2013), arXiv:1302.6263 [hep-ex].
- [73] M. Tanabashi *et al.* (Particle Data Group), *Phys. Rev. D* **98**, 030001 (2018).
- [74] C. J. Horowitz *et al.*, *Phys. Rev. C* **85**, 032501 (2012), arXiv:1202.1468 [nucl-ex].
- [75] R. H. Helm, *Phys. Rev.* **104**, 1466 (1956).
- [76] J. Piekarewicz, A. R. Linero, P. Giuliani, and E. Chicksen, *Phys. Rev. C* **94**, 034316 (2016), arXiv:1604.07799 [nucl-th].
- [77] M. Rosen, R. Raphael, and H. Überall, *Phys. Rev.* **163**, 927 (1967).
- [78] R. Raphael and M. Rosen, *Phys. Rev. C* **1**, 547 (1970).
- [79] A. Ong, J. C. Berengut, and V. V. Flambaum, *Phys. Rev. C* **82**, 014320 (2010), arXiv:1006.5508 [nucl-th].
- [80] H.-W. Hammer and U.-G. Meißner, *Sci. Bull.* **65**, 257 (2020), arXiv:1912.03881 [hep-ph].
- [81] C. J. Horowitz, *Phys. Lett. B* **789**, 675 (2019), arXiv:1809.06478 [nucl-th].
- [82] J. Green, S. Meinel, M. Engelhardt, S. Krieg, J. Laeuchli, J. Negele, K. Orginos, A. Pochinsky, and S. Syritsyn, *Phys. Rev. D* **92**, 031501 (2015), arXiv:1505.01803 [hep-lat].
- [83] M. Wang, W. J. Huang, F. G. Kondev, G. Audi, and S. Naimi, *Chin. Phys. C* **45**, 030003 (2021).
- [84] J. Meija, T. B. Coplen, M. Berglund, W. A. Brand, P. D. Bièvre, M. Gröning, N. E. Holden, J. Irrgeher, R. D. Loss, T. Walczyk, and T. Prohaska, *Pure and Applied Chemistry* **88**, 293 (2016).
- [85] H. Nagakura and K. Hotokezaka, *Mon. Not. Roy. Astron. Soc.* **502**, 89 (2021), arXiv:2010.15136 [astro-ph.HE].
- [86] B. C. Cañas, E. A. Garcés, O. G. Miranda, and A. Parada, *Phys. Lett. B* **784**, 159 (2018), arXiv:1806.01310 [hep-ph].
- [87] M. Mukhopadhyay, C. Lunardini, F. X. Timmes, and K. Zuber, *Astrophys. J.* **899**, 153 (2020), arXiv:2004.02045 [astro-ph.HE].
- [88] L.-S. The, D. D. Clayton, R. Diehl, D. H. Hartmann, A. F. Iyudin, M. D. Leising, B. S. Meyer, Y. Motizuki, and V. Schonfelder, *Astron. Astrophys.* **450**, 1037 (2006), arXiv:astro-ph/0601039.
- [89] J. Vink, in *Handbook of Supernovae*, edited by A. W. Alsabti and P. Murdin (2017) p. 139.
- [90] K. Scholberg, *J. Phys. G* **45**, 014002 (2018), arXiv:1707.06384 [hep-ex].
- [91] B. Hu *et al.*, *Nature Phys.* **18**, 1196 (2022), arXiv:2112.01125 [nucl-th].
- [92] J. Aalbers *et al.*, (2022), arXiv:2203.02309 [physics.ins-det].